

# Journal of Biomedical Optics

[SPIEDigitalLibrary.org/jbo](http://SPIEDigitalLibrary.org/jbo)

## **Laser-induced modifications of gold nanoparticles and their cytotoxic effect**

Shimaa Abdelhamid  
Hazem Saleh  
Mahmoud Abdelhamid  
Adel Gohar  
Tareq Youssef

# Laser-induced modifications of gold nanoparticles and their cytotoxic effect

Shimaa Abdelhamid,<sup>a</sup> Hazem Saleh,<sup>a</sup> Mahmoud Abdelhamid,<sup>a</sup> Adel Gohar,<sup>b</sup> and Tareq Youssef<sup>a</sup>

<sup>a</sup>Cairo University, National Institute of Laser Enhanced Sciences, 12613 Giza, Egypt

<sup>b</sup>Cairo University, Faculty of Veterinary Medicine, 12613 Giza, Egypt

**Abstract.** As nanotechnology continues to develop, an assessment of nanoparticles' toxicity becomes very crucial for biomedical applications. The current study examines the deleterious effects of pre-irradiated gold nanoparticles (GNPs) solutions on primary rat kidney cells (PRKCs). Spectroscopic and transmission electron microscopic studies demonstrated that exposure of 15 nm GNPs in size to pulsed laser caused a reduction both in optical density and mean particle diameter. GNPs showed an aggregation when added to the cell culture medium (DMEM). This aggregation was markedly decreased upon adding serum to the medium. Under our experimental conditions, trypan blue and MTT assays revealed no significant changes in cell viability when PRKCs were incubated with non-irradiated GNPs over a period of 72 h and up to 4 nM GNPs concentration. On the contrary, when cells were incubated with irradiated GNPs a significant reduction in PRKCs viability was revealed. © 2012 Society of Photo-Optical Instrumentation Engineers (SPIE). [DOI: 10.1117/1.JBO.17.6.068001]

Keywords: laser; gold nanoparticles; cytotoxicity; primary rat kidney cells.

Paper 11787 received Dec. 23, 2011; revised manuscript received Apr. 24, 2012; accepted for publication Apr. 24, 2012; published online Jun. 5, 2012.

## 1 Introduction

Nanoscience and nanotechnology hold great promise for many potential applications, including biomedical uses. At a nanoscale size, noble metals and in particularly gold nanoparticles (GNPs) have received a widespread interest in molecular imaging, molecular diagnosis and targeted therapy of malignant tumors due to their easy and fast synthesis, photostability, ability to be taken up into the cell, and the unique optical and electronic properties that are not observed on the bulk scale.<sup>1-7</sup> Spherical GNPs, with diameters much smaller than the wavelength of the incident light, can exhibit intense absorptions in the visible region owing to the high resonant coherent oscillations of the free electrons within this frequency range. Such a phenomenon is known as a surface plasmon resonance (SPR), which depends on the size and shape of the particles, the dielectric constant of the metal and the surrounding medium.<sup>8,9</sup> It has been reported that GNPs, activated by laser irradiation with the appropriate wavelength, can act as efficient photothermal agents mediating cancer therapy, the process in which the absorbed photons are converted to a thermal energy sufficient to induce cellular destruction.<sup>10-12</sup>

Despite the technological advancements of using lasers in photothermal therapy for cells treated with GNPs, a serious lack of information concerns the potential deleterious effects on human and environmental health resulting from laser-GNPs interaction. The modified forms of nanoparticles following exposure to laser may, then, play a significant role in cellular toxicity.

It is well known that kidneys are the major eliminator of toxic compounds and their metabolites from mammalian bodies, thus they are frequently a target of toxic injury. Systemic administration of GNPs in experimental animals demonstrated that clearance of the particles was via the kidneys with a gradual

significant accumulation inside this organ.<sup>13,14</sup> In the present work, the emergences of toxic effects of pulsed laser-induced modifications in 15 nm GNPs were carried out on primary rat kidney cells (PRKCs), as an investigating model, in comparison with non-irradiated GNPs.

## 2 Materials and Methods

### 2.1 Synthesis of GNPs

GNPs were prepared by citrate reduction of Gold (III) chloride trihydrate following the method of Turkevich et al.,<sup>15</sup> which was later refined by Frens.<sup>16</sup> Before the reduction process, all glassware was cleaned in aqua regia (3 parts HCl:1 part HNO<sub>3</sub>), rinsed with deionized H<sub>2</sub>O and then dried. An aqueous solution of Gold (III) chloride trihydrate (HAuCl<sub>4</sub>·3H<sub>2</sub>O) from Sigma-Aldrich USA, (100 ml, 1 mM) was brought to a boiling condition and stirred continuously then a solution of 38.8 mM sodium citrate tribasic dihydrate (C<sub>6</sub>H<sub>5</sub>Na<sub>3</sub>O<sub>7</sub>·2H<sub>2</sub>O) from Sigma-Aldrich USA, was added quickly all at once, resulting in a change in solution color from pale yellow to black to deep red. GNPs were diluted in deionized water and the quality and size of the prepared nanoparticles were investigated using UV-Vis spectrophotometry (T80<sup>+</sup> PG instruments) and transmission electron microscopy (TEM, JEOL JEM-2100) equipped with GATAN CCD Camera (Orius SC200).

### 2.2 Irradiation Procedure

Laser irradiation was done in a rectangular quartz cell of 1 × 1 × 4 cm<sup>3</sup> containing 2 ml of GNPs in aqueous solution under agitation using magnetic stirrer. Samples were irradiated with the second harmonic Q-switched Nd:YAG laser (Brio, Quantel, France) at 532 nm providing pulses of 5 ns duration and a repetition rate of 10 Hz. This wavelength falls around the absorption peak of

Address all correspondence to: Tareq Youssef, Cairo University, National Institute of Laser Enhanced Sciences, Gamma Street, P.O. 12613, Giza, Egypt. Tel: +202 3567 52 62; Fax: +202 3572 94 99; E-mail: tareq.youssef@niles.edu.eg

GNPs, which is ascribed as the surface plasmon absorption of gold particles. The laser beam cross-section was determined by the burned pattern printed on a thermal recording paper, and was typically  $0.2 \text{ cm}^2$ . The laser pulse energy was measured in front of the cell using a Joulmeter (SCIENTECH, Model AC5001, USA energy meter) and estimated to be 50 mJ. Samples were irradiated for 3 and 5 min, then the optical and morphological changes of the irradiated GNPs were examined using UV-Vis spectroscopy and TEM.

### 2.3 Primary Rat Kidney Cell Culture

Kidneys were taken after dissection of rats (100 to 120 g in weight), as obtained from the animal house of Research Institute of Ophthalmology (Egypt). All animal procedures and care were performed following guidelines for the Care and Use of Laboratory Animals<sup>17</sup> and approved by the Animal Ethics Committee at Cairo University. The kidneys were placed in alcohol for surface sterilization, then transferred into the cell culture medium ("DMEM" Dulbecco's modified Eagle's medium from Lonza Bioproducts, Belgium) containing 10% fetal bovine serum "FBS" (Gibco, Invitrogen Life technologies, CA-USA) and 1% penicillin streptomycin (purchased from Lonza Bioproducts, Belgium), then their capsules were removed. The kidneys were cut into small fragments and transferred into a glass homogenizer containing the culture media to convert tissue to cell suspension. The cell count was done using hemocytometer (Clay Adams, New York, USA). Appropriate volumes from cell suspension were placed into tissue culture plates and then incubated in a humidified atmosphere of 95% air, 5%  $\text{CO}_2$  at  $37^\circ\text{C}$ .

### 2.4 Effect of Cell Culture Medium on GNPs Stability

The effect of cell culture medium (DMEM) on the optical properties and aggregation state of GNPs co-cultured with DMEM was investigated using UV-Vis spectroscopy and TEM. In order to mimic the proper environmental conditions for cell growth that normally comprise a small proportion of serum in DMEM, spectrophotometric and TEM studies were also proceeded on GNPs in DMEM containing 10% FBS.

### 2.5 In Vitro Cytotoxicity Studies

In order to explore the *in vitro* cytotoxicity of laser irradiated GNPs in comparison with non-irradiated particles on PRKCs, two cytotoxicity assays have been employed; including trypan blue (TB) and 3-(4, 5-dimethylthiazol-2-yl)-2, 5-diphenyl tetrazolium bromide (MTT). The influence of different parameters on cell toxicity was investigated by varying the irradiation time of GNPs, GNPs concentration, and the incubation period of cells with GNPs. Cells incubated in culture medium without GNPs representing 100% viability were included as a negative control. All measurements were repeated three times.

#### 2.5.1 Trypan blue assay

Cell viability was investigated by staining the cells with trypan blue dye. The dead cells accumulated trypan blue and became blue in color while the viable cells repelled the dye and were seen colorless. Under our experimental conditions, approximately  $1 \times 10^5$  cells were seeded per well in 24-well tissue culture plates and incubated in a  $\text{CO}_2$  incubator at  $37^\circ\text{C}$  forming a confluence sheet. Non-irradiated and irradiated GNPs for 3 and 5 min were incubated with PRKCs at different

concentrations (1, 2, and 4 nM) for different incubation periods (24, 48, and 72 h). After each experimental condition, cells were harvested and then equal volumes of cell suspension in PBS and 0.4% trypan blue (BIO BASIC INC, Toronto, Canada) were mixed and left for 2 min at room temperature. Then cells were counted under a microscope.

#### 2.5.2 MTT assay

The MTT assay helps in cell-viability assessment by measuring the enzymatic reduction of yellow tetrazolium MTT to a purple formazan. Approximately,  $1 \times 10^4$  cells were seeded per well in 96-well tissue culture plates and were incubated in a  $\text{CO}_2$  incubator at  $37^\circ\text{C}$  forming a confluence sheet. Non-irradiated and irradiated GNPs for 3 and 5 min were incubated with PRKCs at different concentrations (1, 2, and 4 nM) for different incubation periods (24, 48, and 72 h). After each experimental condition, the medium was discarded and  $50 \mu\text{l}$  of fresh tetrazolium MTT solution, at a concentration of 5 mg/ml in PBS, was added to each well and then incubated for another 1 h at  $37^\circ\text{C}$ . The supernatant was removed and  $200 \mu\text{l}$  dimethyl sulfoxide (DMSO) was added to each well and incubated for 10 min before spectrophotometric measurements.<sup>18</sup> The spectrophotometric absorbance of the reduced MTT was measured in a microtiter plate reader at a test wavelength 570 nm (Microplate Biokinetics Reader, EL 340, BIO-TEK™ instruments, USA) to obtain the optical density (OD) for every well. The percentage of cell viability was calculated according to the following equation:

$$\text{Cell viability}\% = \left( \frac{\text{mean of OD of treated cells with GNPs}}{\text{mean OD of controls}} \right) \times 100.$$

### 2.6 Statistical Analysis

Values of cell viability are expressed as the mean  $\pm$  S.D and the significance of the differences, relative to control, was

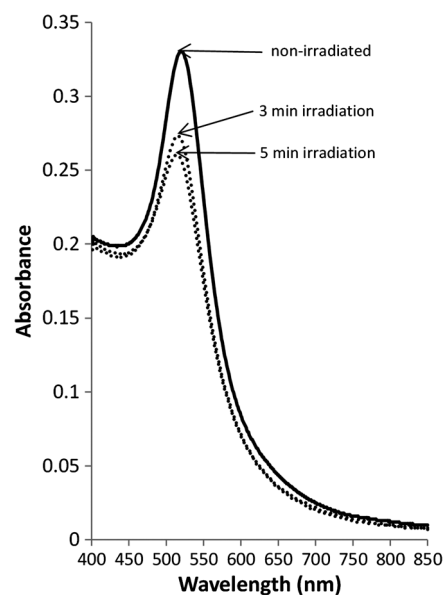


**Fig. 1** Absorption spectra of the prepared GNPs in aqueous medium before and after exposure to 532 nm pulsed laser for 3 and 5 min (fluence  $250 \text{ mJ cm}^{-2}$ ).

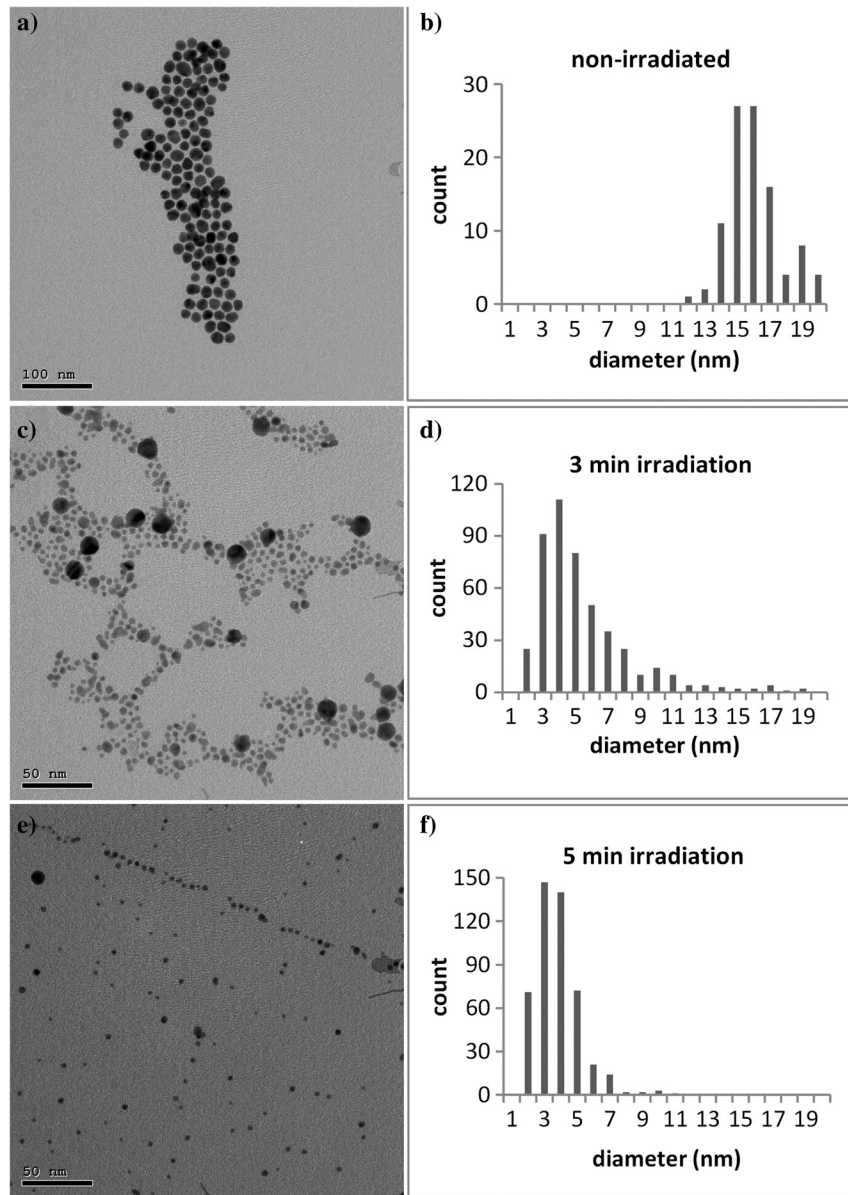


**Fig. 2** TEM micrographs and histograms of GNPs size distribution. (a and b) TEM image (scale bar 100 nm) and size distribution of GNPs before irradiation. (c and d) TEM image (scale bar 50 nm) and size distribution of GNPs after 3 min irradiation. (e and f) TEM image (scale bar 50 nm) and size distribution of GNPs after 5 min irradiation. Irradiation was done using Nd:YAG laser with a second harmonic at 532 nm (fluence 250 mJ cm<sup>-2</sup>).

calculated by Student's *t*-test using SPSS (version 15). Values of  $p < 0.05$  were considered as significant.

### 3 Results

#### 3.1 Effect of Laser Irradiation on GNPs

The effect of laser irradiation on GNPs size was examined in aqueous solution after irradiation with 532 nm pulsed laser for 3 and 5 min exposure time. Figure 1 shows the absorption spectra of irradiated GNPs, recorded in the visible range, in comparison with non-irradiated GNPs. The characteristic GNPs absorption peak, due to the surface plasmon resonance, was found at 520 nm for a non-irradiated sample. After 3 and 5 min irradiation, spectra exhibited blue shifts from 520 to 515, and 513 nm respectively accompanied with a decrease in the

optical density with about 18% and 22% with respect to non-irradiated samples.

Figure 2 illustrates TEM micrographs of GNPs in aqueous medium and particle size distribution before irradiation and after 3 and 5 min exposure to laser pulses. The formation of spherical GNPs was shown in Fig. 2(a). Size distribution analysis using TEM clearly showed that particles mostly reside within a 15 nm size range [Fig. 2(b)]. This average particle size come in a very good agreement with the calibration curve performed on different nanoparticle sizes as a function of the peak wavelength of the SPR in comparison with Mie theory.<sup>19</sup> After 3 min irradiation, it was estimated that about 95% of particles population was exposed to a reduction in size with an average diameter 4 nm [Fig. 2(c) and 2(d)]. In the case of 5 min irradiation, more than 99% of particles population was reduced to an average size 3 nm [Fig. 2(e) and 2(f)].

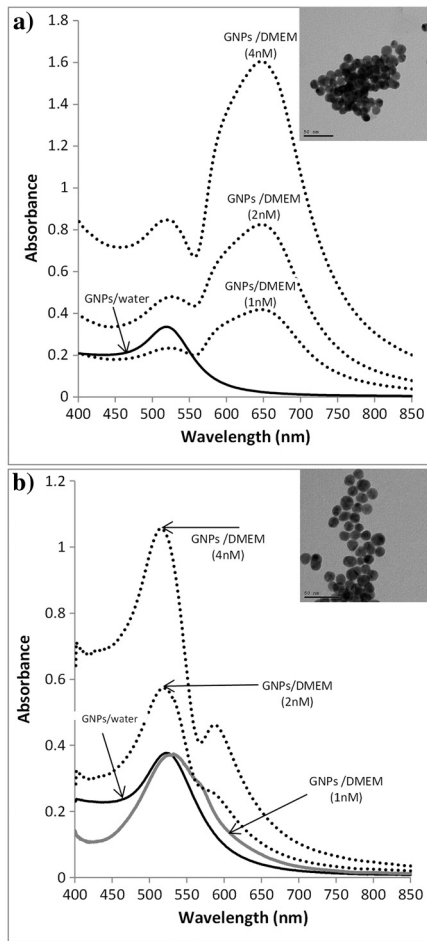


**Fig. 3** Absorption spectra of GNPs at different concentrations. (a) In DMEM, the inset represents the TEM micrograph of the aggregation state of 4 nM GNPs (scale bar 50 nm). (b) In DMEM containing 10% serum, the inset represents the TEM micrograph of 4 nM GNPs with improved dispersion (scale bar 50 nm).

### 3.2 Effect of Cell Culture Medium on GNPs

In order to make sure that the cytotoxic effect is due to laser-induced modification to GNPs rather than other influences from the surrounding medium, spectrophotometric and TEM studies were proceeded on GNPs samples in DMEM and in DMEM containing a small proportion of fetal bovine serum. Figure 3(a) shows the absorption spectra of various concentrations of GNPs (1, 2, and 4 nM) in DMEM in comparison with GNPs in water (1 nM). Spectra showed an appearance of a new peak at a longer wavelength (around 646 nm), which increases with the increase of particles concentrations suggesting an aggregation of the particles. TEM image for 4 nM GNPs gives an evidence for the aggregation state [inset of Fig. 3(a)]. Figure 3(b) demonstrates the effect of DMEM containing 10% serum on the absorption spectra of GNPs with different concentrations (1, 2, and 4 nM) in comparison with GNPs in water (1 nM). At 1 nM, the absorption spectrum demonstrated a slightly broad band with a red shift of about 10 nm at the maximum peak, from 520 nm for GNPs in water to 530 nm in the culture medium. On the contrary, at 2 nM, the spectrum showed a slight blue shift to 518 nm with the appearance of a shoulder at a longer wavelength (around 588 nm). At a higher concentration (4 nM), the spectrum

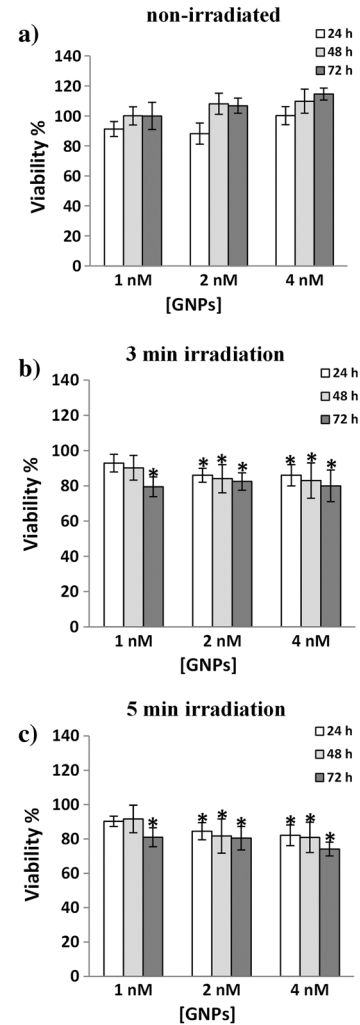


**Fig. 4** Viability percent of PRKCs (mean values  $\pm$  S.D) using trypan blue assay, measured after incubation with 1, 2 and 4 nM GNPs for different incubation times (24, 48 and 72 h). (a) Non-irradiated GNPs. (b) 3 min irradiated GNPs. (c) 5 min irradiated GNPs. (\*) indicates a statistically significant difference compared with control ( $p < 0.05$ ).

showed a more blue shift with a maximum peak at 515 nm and a more pronounced peak around 588 nm. TEM image for 4 nM GNPs showed a marked decrease in GNPs aggregation even though some particles come close to each other having the tendency to aggregate [inset of Fig. 3(b)].

### 3.3 In vitro Cytotoxicity Assessment

#### 3.3.1 Trypan blue assay

When PRKCs were incubated with non-irradiated GNPs, cells showed insignificant increases in cell viability after 48 and 72 h incubation with 2 and 4 nM of GNPs concentration ( $p > 0.05$ ) as shown in Fig. 4(a). On the contrary, when cells were incubated with irradiated GNPs, a reduction in cell viability was noticed. After 3 and 5 min irradiation [Fig. 4(b) and 4(c) respectively], a significant reduction in cell viability was detected at 1 nM GNPs after 72 h incubation and at 2 and 4 nM GNPs after 24, 48, and 72 h incubation ( $p < 0.05$ ).

### 3.3.2 MTT assay

When cells were incubated with non-irradiated GNPs, cells showed insignificant decreases in PRKCs viability up to 72 h incubation for all concentrations used ( $p > 0.05$ ) as shown in Fig. 5(a). After 3 and 5 min irradiation [Fig. 5(b) and 5(c) respectively], a significant reduction in cell viability was shown after 48 and 72 h incubation for all concentrations used ( $p < 0.05$ ).

## 4 Discussion

The present study investigates the emergences of toxic effects of pulsed laser-induced GNPs modifications on PRKCs. Both

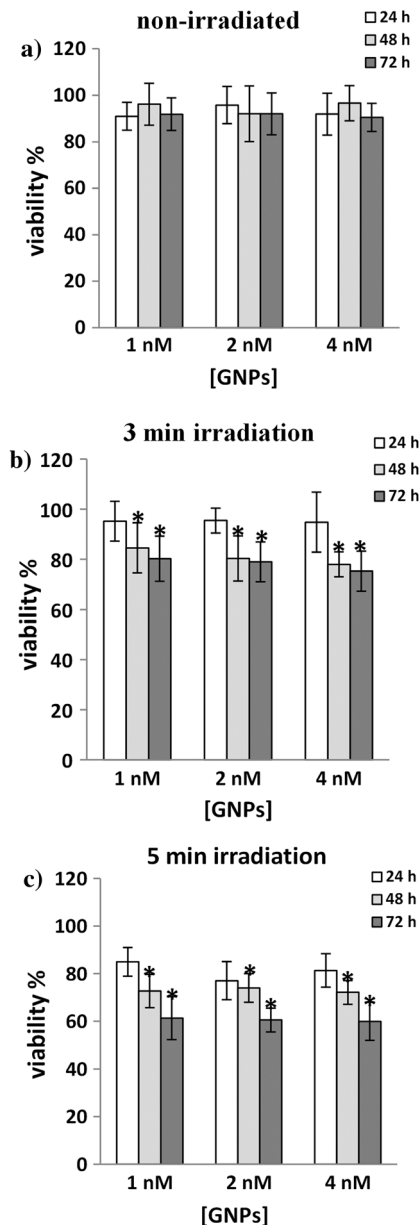


**Fig. 5** Viability percent of PRKCs (mean values  $\pm$  S.D.) using MTT assay, measured after incubation with 1, 2 and 4 nM GNPs for different incubation times (24, 48 and 72 h). (a) Non-irradiated GNPs. (b) 3 min irradiated GNPs. (c) 5 min irradiated GNPs. (\*) indicates a statistically significant difference compared with control ( $p < 0.05$ ).

spectroscopic and TEM studies demonstrated that exposure of 15 nm GNPs in size to 532 nm pulsed laser caused a reduction both in optical density and mean particle diameter, depending on the time of irradiation. Exposure for 3 and 5 min showed a reduction in optical density with about 18% and 22% respectively in comparison with non-irradiated samples. Also, blue shifts in the plasmon band with about 5 and 7 nm were detected after 3 and 5 min irradiation respectively, which is an indication of particle size reduction. Particle size distribution demonstrated that large particles disappeared and became typically spherical with smaller diameters following irradiation. The average diameter was shifted from 15 nm for non-irradiated GNPs to smaller particles diameters with 4 and 3 nm following 3 and 5 min irradiation respectively [Fig. 2(b), 2(d) and 2(f)]. As reported by some authors,<sup>20–22</sup> particle size reduction following pulsed laser irradiation can mainly be attributed to photo-thermal process resulting in vaporization of the gold particle. When the temperature of the gold particle rises to the boiling point, atoms and/or small particles are ejected through vaporization, resulting in particle size reduction. This process was referred as photofragmentation, which depends on the optical absorbance cross-section of nanoparticles, laser fluence, pulse duration and the rate of heat transfer between the nanoparticle and surrounding media.<sup>20–23</sup> Transient absorption spectroscopy of the femtosecond laser-induced size fragmentation of 60 nm diameter aqueous GNPs revealed fragmentation is possible at picosecond time scales.<sup>24</sup> Also, photothermal shape modification of GNPs in micellar solution from nano-rods to nano-spherical was demonstrated after exposure to femtosecond laser pulses.<sup>25</sup>

Investigating the effect of cell culture medium on the optical and morphological properties of GNPs, our results demonstrated that particles exhibited a strong aggregation when added to the cell culture medium “DMEM” [Fig. 3(a)]. The appearance of a new peak at a longer wavelength that intensifies with the increase of GNPs concentration suggests the formation of particles aggregation. TEM image for 4 nM GNPs in DMEM confirms this aggregation state [inset of Fig. 3(a)], which was mainly attributed to the high concentration of sodium salt in the medium, reducing the electrostatic repulsion between the particles.<sup>18,26</sup> Upon adding serum to the medium, the interparticles spacing was obviously increased and GNPs showed improved dispersion in the medium. Particles in this case were suggested to be coated with serum where the surface of GNPs was modified by non-specific adsorption of serum proteins. This is likely since citric acid stabilizers are weakly bound to the surface of GNPs and could be desorbed from the metal surfaces by proteins.<sup>26–28</sup> On the other hand, the optical absorption spectra of 2 and 4 nM GNPs in DMEM containing serum showed blue shifts in their plasmon band compared with GNPs in water. Those blue shifts were accompanied with the appearance of low intensity absorption peaks at a longer wavelength, which is an indication of anisotropic feature of some GNPs [Fig. 3(b)]. TEM image of 4 nM GNPs in DMEM in the presence of serum [inset of Fig. 3(b)] indicates the formation of few non-spherical particles compared with GNPs dispersed in aqueous medium [Fig. 2(a)] where some particles have the tendency to aggregate resulting from a decrease in GNPs stability.<sup>29,30</sup> In fact, the optical properties of the metallic nanoparticles are mainly determined by two contributions: the properties of the particles acting as well-isolated individuals and the collective properties of the whole ensemble. When

individual spherical GNPs come into close proximity to one another, the interparticle coupling becomes more effective depending on size and shape of the formed aggregates (Ref. 31 and references therein).

The *in vitro* cytotoxicity assays demonstrated that non-irradiated GNPs with an average size of 15 nm revealed no significant changes on PRKCs viability over a period of 72 h incubation and up to the highest concentration used of GNPs (4 nM). These findings come in a good agreement with other studies which reported that particles within this size range are insignificantly toxic.<sup>26</sup> On the contrary, when cells were incubated with irradiated GNPs for 3 and 5 min, a pronounced reduction in PRKCs viability was shown. This effect was demonstrated by the significant decreases in the percent of viable cells using trypan blue and MTT assays. The decreases in cell viability became more pronounced at 4 nM GNPs and after 72 h incubation [Figs. 4 and 5]. Although cytotoxicity of GNPs is gaining more attention in evaluating the potential biomedical applications of GNPs, there are still challenging debates about the size dependent cell toxicity. Based on the study by Pan et al.,<sup>32</sup> and Fan et al.,<sup>33</sup> who investigated the cytotoxic effects of a wide range of GNPs up to 15 and 30 nm in size on different cell lines, particles with size ranges less than 5 nm showed higher toxicity than 15 or 30 nm. Similarly Yen et al.,<sup>34</sup> demonstrated that the cytotoxicity to macrophages with GNPs of smaller size ranges 2 to 4 nm was more pronounced than those particles with size ranges 5 to 7 nm or 20 to 40 nm.

In this work, the formation of smaller particle sizes (<5 nm) resulting from pulsed laser irradiation may contribute to the enhanced toxicity of PRKCs when compared with non-irradiated GNPs of 15 nm in size. As suggested by Zharov et al.,<sup>35</sup> photofragmentation of GNPs could play a role in cell killing mechanism. However, work is still in progress in order to investigate the formation of other cytotoxic species following laser irradiation (e.g. release of gold ions).

## 5 Conclusion

As GNPs are amenable to be used for photothermal therapy of several serious diseases, an assessment of nanoparticles toxicity resulting from laser-induced particles modifications should be seriously considered. Literature reviews showed a wide range of conflicting data regarding the cytotoxicity of size dependent of GNPs. The modified forms of nanoparticles following exposure to laser can play a significant role in cellular toxicity as they can show distinct optical characteristics and can be also expected to express different biodistribution in living tissues.

## Acknowledgments

This work was kindly supported by a grant from Cairo University-Egypt.

## References

- X. Huang, P. K. Jain, and I. H. El-Sayed, "Plasmonic photothermal therapy (PPTT) using gold nanoparticles," *Lasers Med. Sci.* **23**(3), 217–228 (2008).
- X. Huang, I. H. El-Sayed, and M. A. El-Sayed, "Cancer cell imaging and photothermal therapy in the near infrared region by using gold nanorods," *J. Am. Chem. Soc.* **128**(6), 2115–2120 (2006).
- E. E. Connor et al., "Gold nanoparticles are taken up by human cells but do not cause acute cytotoxicity," *Small* **1**(3), 325–327 (2005).<http://onlinelibrary.wiley.com/doi/10.1002/sml.200400093/abstract>
- L. B. Peppas and J. O. Blanchette, "Nanoparticle and targeted systems for cancer therapy," *Adv. Drug Deliv. Rev.* **56**(11), 1649–1659 (2004).
- N. Elbially, M. Abdelhamid, and T. Youssef, "Low power argon laser-induced thermal therapy for subcutaneous Ehrlich carcinoma in mice using spherical gold nanoparticles," *J. Biomed. Nanotechnol.* **6**(6), 687–693 (2010).
- H. K. Patra et al., "Cell-selective response to gold nanoparticles," *Nanomedicine* **3**(2), 111–119 (2009).<http://www.ncbi.nlm.nih.gov/pubmed/17572353>
- W. N. Rahman et al., "Enhancement of radiation effects by gold nanoparticles for superficial radiation therapy," *Nanomedicine* **5**(2), 136–142 (2009).
- K. L. Kelly et al., "The optical properties of metal nanoparticles: the influence of the size, shape and dielectric environment," *J. Phys. Chem. B* **107**(3), 668–677 (2003).
- M. A. El-Sayed, "Some interesting properties of metals confined in time and nanometer space of different shapes," *Acc. Chem. Res.* **34**(4), 257–264 (2001).
- W. Cai et al., "Applications of gold nanoparticles in cancer nanotechnology," *Nanotechnol. Sci. Appl.* **1**, 17–32 (2008).<http://www.dovepress.com/applications-of-gold-nanoparticles-in-cancer-nanotechnology-peer-reviewed-article-NSA-MVP>
- X. Huang et al., "Gold nanoparticles: interesting optical properties and recent applications in cancer diagnostics and therapy," *Nanomedicine* **2**(5), 681–693 (2007).
- E. B. Dickerson et al., "Gold nanorod assisted near-infrared plasmonic photothermal therapy (PPTT) of squamous cell carcinoma in mice," *Cancer Lett.* **269**(1), 57–66 (2008).
- S. K. Balasubramanian et al., "Biodistribution of gold nanoparticles and gene expression changes in the liver and spleen after intravenous administration in rats," *Biomaterials* **31**(8), 2034–2042 (2010).
- J. F. Hainfeld et al., "Gold nanoparticles: a new X-ray contrast agent," *Br. J. Radiol.* **79**(939), 248–253 (2006).
- J. Turkevich, P. C. Stevenson, and J. A. Hillier, "A study of the nucleation and growth processes in the synthesis of colloidal gold," *Discuss. Faraday Soc.* **11**, 55–75 (1951).<http://pubs.rsc.org/en/content/articlelanding/1951/df/d9511100055>
- G. Frens, "Controlled nucleation for the regulation of particle size in monodisperse gold suspensions," *Nat. Phys. Sci.* **241**, 20–22 (1973). <http://www.nature.com/nature-physics/journal/v241/n105/abs/physci241020a0.html>
- National Research Council, *Guide for the Care and Use of Laboratory Animals*, National Academy Press, Washington, DC (1996).
- S. Wang et al., "Challenge in understanding size and shape dependent toxicity of gold nanomaterials in human skin keratinocytes," *Chem. Phys. Lett.* **463**(1–3), 145–149 (2008).
- J. Kimling et al., "Turkevich method for gold nanoparticle synthesis revisited," *J. Phys. Chem. B* **110**(32), 15700–15707 (2006).
- O. Dammer et al., "Interaction of high-power laser pulses with monodisperse gold particles," *Mater. Sci. Eng. B* **140**(3), 138–146 (2007).<http://www.sciencedirect.com/science/article/pii/S0921510707001407>
- H. Kurita, A. Takami, and S. Koda, "Size reduction of gold particles in aqueous solution by pulsed laser irradiation," *Appl. Phys. Lett.* **72**(7), 789–791 (1998).
- A. Takami, H. Kurita, and S. Koda, "Laser-induced size reduction of noble metal particles," *J. Phys. Chem. B* **103**(8), 1226–1232 (1999).
- S. Inasawa, M. Sugiyama, and S. Koda, "Size controlled formation of gold nanoparticles using photochemical growth and photothermal size reduction by 308 nm laser pulses," *Jpn. J. Appl. Phys.* **42**(10), 6705–6712 (2003).
- D. Werner et al., "Femtosecond laser-induced size reduction of aqueous gold nanoparticles: in situ and pump probe spectroscopy investigations revealing coulomb explosion," *J. Phys. Chem. C* **115**(17), 8503–8512 (2011).
- S. Link et al., "Laser photothermal melting and fragmentation of gold nanorods: energy and laser pulse-width dependence," *J. Phys. Chem. A* **103**(9), 1165–1170 (1999).
- D. Mahl et al., "Gold nanoparticles: dispersibility in biological media and cell-biological effect," *J. Mater. Chem.* **20**(29), 6176–6181 (2010).

27. B. D. Chithrani, A. A. Ghazani, and W. C. Chan, "Determining the size and shape dependence of gold nanoparticle uptake into mammalian cells," *Nano Lett.* **6**(4), 662–668 (2006).
28. M. A. Dobrovolskaia, A. K. Patri, and J. Zheng, "Interaction of colloidal gold nanoparticles with human blood: effects on particle size and analysis of plasma protein binding profiles," *Nanomedicine* **5**(2), 106–117 (2009).
29. C. Wang et al., "Aqueous gold nanosols stabilized by electrostatic protection generated by X-ray irradiation assisted radical reduction," *Mater. Chem. Phys.* **106**(2–3), 323–329 (2007).
30. C. Wang et al., "Optimizing the size and surface properties of polyethylene glycol (PEG)-gold nanoparticles by intense x-ray irradiation," *J. Phys. D* **41**(19), 195301–195309 (2008).
31. S. Basu et al., "Biomolecule induced nanoparticle aggregation: effect of particle size on interparticle coupling," *J. Colloid Interface Sci.* **313**(2), 724–734 (2007).
32. Y. Pan et al., "Size-dependent cytotoxicity of gold nanoparticles," *Small* **3**(11), 1941–1949 (2007).<http://www.ncbi.nlm.nih.gov/pubmed/17963284>
33. J. H. Fan et al., "Biocompatibility study of gold nanoparticles to human cells," in *13th International Conference on Biomedical Engineering IFMBE Proc.*, Vol. **23**, pp. 870–873, Springer, Singapore (2009).<http://www.springerlink.com/content/x0hg168k51004326/>
34. H. J. Yen, S. H. Hsu, and C. L. Tsai, "Cytotoxicity and immunological response of gold and silver nanoparticles of different sizes," *Small* **5**(13), 1553–1561 (2009).<http://www.ncbi.nlm.nih.gov/pubmed/19326357>
35. V. P. Zharov, V. Galitovsly, and M. Viegas, "Photothermal guidance of selective photothermolysis with nanoparticles," *Proc. SPIE* **5319**, 291–300 (2004).